AIAA SciTech
13-17 January 2014, National Harbor, Maryland
52nd Aerospace Sciences Meeting

Flow Control over a Conical Forebody Using Pulsed Nanosecond Discharge Actuators

Yuexiao Long[1], Huaxing Li[2], Xuanshi Meng[3],

(*1. National Key Laboratory of Science and Technology on Aerodynamic Design and Research, Northwestern Polytechnical University, Xi'an 710072, China*)

Feng Liu[4] and Shijun Luo[5]

(*2. The Department of Mechanical and Aerospace Engineering , University of California, CA 92697-3975, America*)

The study of a pair of single Dielectric Barrier Discharge (DBD) plasma actuator which is placed on the surface near the apex of a cone-cylinder body with a semi-apex angle of 10° is presented. The two SDBD plasma actuators are aligned on the cone at azimuth angle θ = ±90° symmetrically and sustained by a repetitive high voltage nanosecond pulses generator. The pressure distribution over the test section is measured through pressure-tappings on the model surface. Based on the features of conical pressure-distribution studied before, the pressure distribution of one cross section could represent the pressure distribution over the entire cone at the angle of attack of 45°. The lateral force of the cone is obtained by integrating the pressure distributions. Tests are performed at 22 m/s and 42 m/s with the Reynolds number 1.64 × 10^5 and 3.09 × 10^5 based on the cone base diameter respectively. The test results show that the port actuation has the opposite effect to the starboard the actuation in changing the pressure distribution. As the wind speed increased, the plasma actuator effect well gradually. The side force of the cone-cylinder model can be manipulated by activating the plasma actuator in the test at 42 m/s.

Nomenclature

C_p	=	pressure coefficient
C_{Yd}	=	time-averaged local side-force coefficient, local side force/$q_\infty d$
D	=	base diameter of circular cone forebody
d	=	local diameter of circular cone forebody
F	=	wave-frequency of NS voltage source
L	=	length of circular cone forebody
q_∞	=	free-stream dynamic pressure
Re	=	free-stream Reynolds number based on the diameter of the cone, $U_\infty D/\nu$
U_∞	=	free-stream velocity
V_{max}	=	maximum voltage of NS voltage source
$V_{p\text{-}p}$	=	peak to peak voltage of AC voltage source
x, y, z	=	body coordinates, x toward base, y toward starboard, right-hand system
α	=	angle of attack
θ	=	meridian angle measured clockwise from windward generator at positive α and looking upstream
ε	=	the turbulivity of the wind tunnel

[1] PHD Student, Department of Fluid Mechanics.
[2] Professor, Department of Fluid Mechanics.
[3] Associate Professor, Department of Fluid Mechanics.
[4] Professor, Department of Mechanical and Aerospace Engineering. Fellow AIAA.
[5] Researcher, Department of Mechanical and Aerospace Engineering

I. Introduction

The vortices are very sensitive to small perturbations near the apex of a forebody at the high angle f attack[1-4]. Although methods have been developed to delay the onset of asymmetric vortex shedding, the fact that the separation vortices generate large airloads and are very sensitive to small perturbations offers an exceptional opportunity for manipulating them with little energy input to achieve active lateral control of the vehicle in place of conventional control surfaces. Methods toward such a goal, by using various deployable mechanical devices and suction and blowing mechanisms, have been studied and reviewed by Malcolm[5] and Williams[6]. Most of these methods are based on steady methods in the sense that the control actuation is through a static or steady excitation.

Plasma active flow control has received growing attention in recent years because of the advantages of not having mechanical parts, zero reaction time, broader frequency bandwidths and relatively low energy consumption. What is most important, the plasma actuators can be arranged conveniently on the parts surface of the vehicle. Many researchers choose the single dielectric barrier discharge (SDBD) as the plasma actuation type. The effect of the SDBD actuator is to impart momentum to the flow, much like flow suction or blowing but without the mass injection. Post and Corke[7,8] successfully demonstrated their use in the control of separation over stationary and oscillating airfoils. Huang et al.[9] also used them to control separation over turbine blades. A review is provided by Corke and Post[10]. Takashi Matsuno et al.[11] used a pair of plasma actuators which located at the $\pm 120^{\circ}$ from the leeward meridian near the nose of a tangent ogive nose cylindrical model to manipulate the forebody vortices. The experiments have confirmed that the plasma actuator can be used to displace the vortex on the forebody model by the Coanda effect. Meng et al.[12] reported wind-tunnel experiments that demonstrated the control of lateral forces to bi-stable over a conical forebody at high angles of attack by a couple of SDBD aligned at the azimuth angle $\theta = \pm 90^{\circ}$ which is powered by a traditional AC generator.

Repetitive nanosecond (NS) pulses generator is a new kind of plasma generator which can provide the actuation with a higher voltage and frequency. The NS-DBD is approximately same as the AC-DBD (Alternative Current), but the effect mechanism is totally different. The Jesse Little et al.[13] have performed the control of the flow on platform and airfoil. They find that the NS-DBD transfers substantially less momentum to the neutral air molecules than the AC-DBD plasma actuator. Instead, the control authority generated by NS-DBD plasma is believed to come from the rapid localized heating of the near-surface gas layer by plasma. They have raised the control wind speed over the airfoil leading edge to 62 m/s. The compression waves generate by localized heat is the key factor to the control of the flow. Keisuke takashima et al.[14] have detect the characterization of the NS-DBD by phase-locked schlieren and the results suggests that the compression wave may be a superposition of individual waves generated by discharge filaments, some of which remain fairly reproducible pulse-to-pulse. The results demonstrate that compression waves generated by discharge filaments have higher amplitude and high speed, compared to those produced in a diffuse discharge.

In this paper, an experimental investigation on SDBD which is aligned on the surface of the conical forebody driven by repetitive nanosecond generator is performed. Before the wind tunnel experiments, we do some basic research on platform and the electric characteristic of the DBD actuator is obtained. The PIV study over the actuator on the platform is also conducted. The two SDBD plasma actuators are aligned with the cone at azimuth angle $\theta = \pm 90^{\circ}$ symmetrically. The experiments are performed at 22 m/s and 42 m/s with the Reynolds number 1.64×10^5 and 3.09×10^5 based on the cone base diameter respectively. Then, the pressure distribution is measured by pressure scanner though 36 pressure-tappings on the model surface arranged around the test section. Finally, the lateral force can be obtained by the integration of the pressure distribution. At 22 m/s, we cannot control the asymmetry vortex by actuating the actuator. But when the wind speed increase to 42 m/s, actuators work well. Even though the separation vortices flow field is not bi-stable after the plasma control, the sign of C_{Yd} for port and starboard on is opposite. This result indicates that the asymmetric lateral force and vortices can be well controlled by activating the NS-DBD actuator at 42 m/s.

II. Experimental and Setup

A. Smoke Wind-Tunnel and Low acoustic Wind-Tunnel

The flow control experiment is performed in a low velocity closed circuit wind tunnel with a circle test section entrance which diameter is 1.5 m and the length of the open test section is 1.9 m. The no-load maximum velocity of the wind tunnel is $U_\infty = 45$ m/s. The cone-cylinder model is tested at $\alpha = 45^{\circ}$ through an angle of attack institution in the chamber either. In experiment, the free stream velocity is $U_\infty = 22$ m/s - 42 m/s with a Reynolds number $Re = (1.64 - 3.09) \times 10^5$ based on the cone base diameter. The blockage radio of the model in smoke wind tunnel is about 1.5%. The turbulivity of the wind tunnel is $\varepsilon \leqq 0.02$ %.

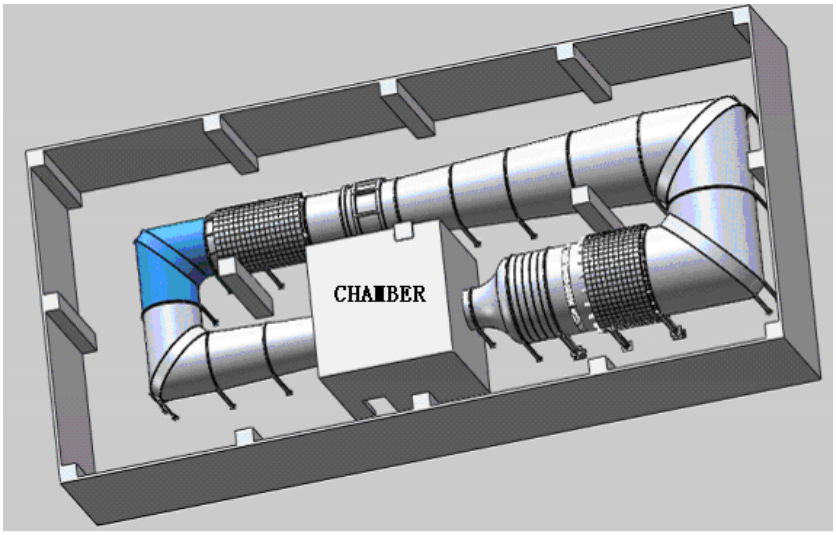

Figure 1. Wind tunnel sketch

B. Conical Forebody Model

The nose of any pointed forebody is locally conical in shape, so the flow may be regarded as locally equivalent to that about a tangent cone. For this reason, a combination of a circular cone with a semi-apex angle of 10 deg and a fairing segment is tested. The whole model is made of plastic to insure the insulation. The total length of the cone is 331.3 mm with a base diameter of 116.83 mm. The fairing segment make the diameter a smooth transition from 116.83 mm to 142.8 mm and the length of it is 140.7 mm. So, the total length of the model is 472 mm.

The time-averaged pressure tapping are arranged in 10° increments around the azimuth of the cone at station 1 (Fig.2). Since the pressure distribution over the forebody at angle of attack of 45° is approximately conical except in the immediate neighborhood of the body apex[15]. So these pressure taps around the circumference of the measured station can be used to detect changes in the direction of side-force and the configuration of the vortices over the forebody of the cone. The model is carefully cleaned prior to each run of the wind tunnel.

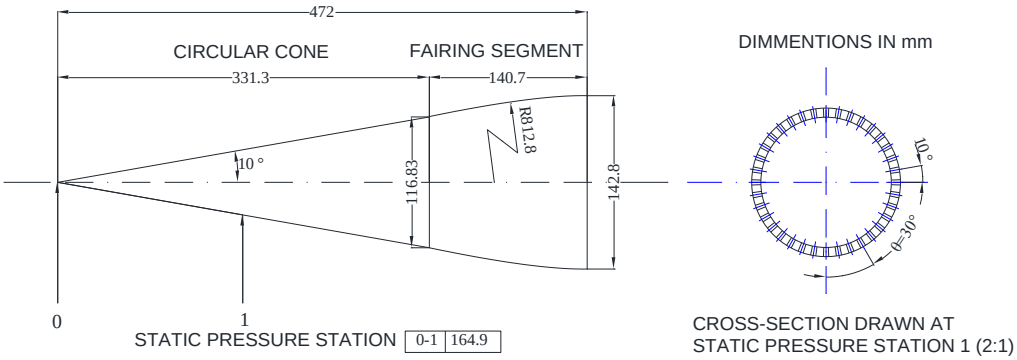

Fig. 2 The model and statistic pressure tappings arrangement sketch

C. Dielectric-Barrier-Discharge Plasma Actuators

On the basis of the previous work, we continue to use the actuator like AC-DBD, but change the thickness of the barrier in case of being punctured by high nanosecond pulse. A pair of long strips of DBD plasma actuator is placed symmetrically on the plastic frontal cone just near the apex as shown in Fig. 3a). The direction which the arrow points to is along the electric potential. The azimuth angle θ of the pressure-tappings is measured from the windward meridian and the clockwise (from the port side to the starboard side) is positive.

The NS-DBD plasma actuator includes two asymmetric copper electrodes which thickness is 0.03 mm and a thin dielectric film which is wrapped around the cone surface and separates the covered electrode from the exposed electrode as shown in Fig. 3b). The thickness of the thin dielectric film is about 0.33mm (6 layers, each layer is 0.055mm). The length of the electrodes is 100 mm along the cone meridian with the leading edge which is 15mm to

the cone apex. The width of the exposed and covered electrode is 2 mm and 10 mm respectively. There is no gap or overlap between the exposed and covered electrode.

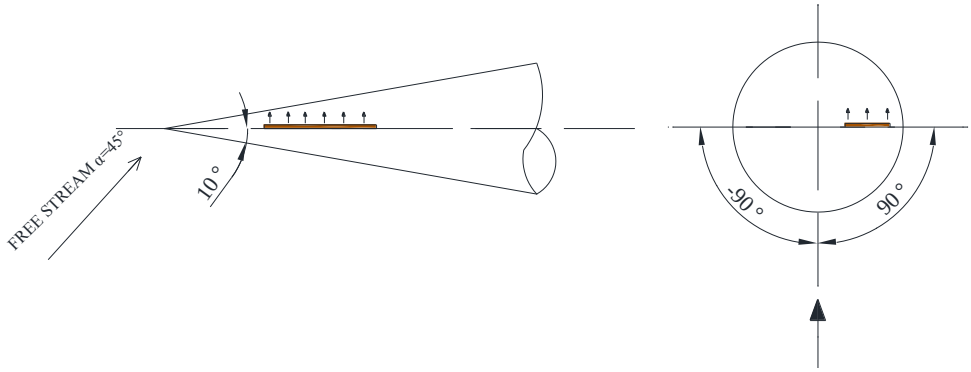

a) Arrangement

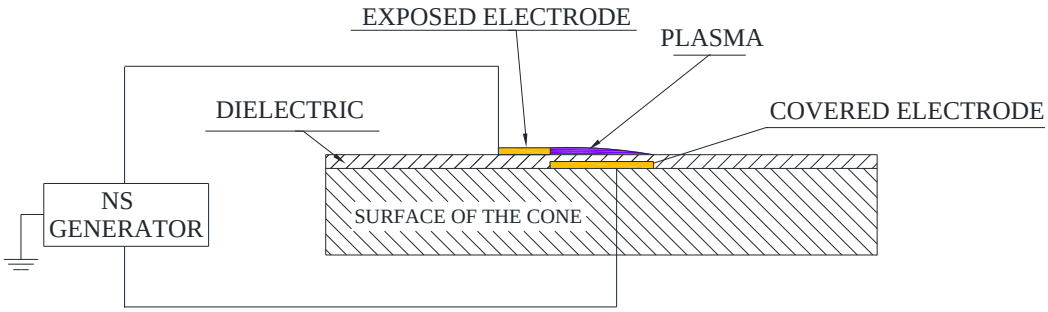

b) Dielectric Barrier Discharge

Figure 3. Sketches of the plasma actuators

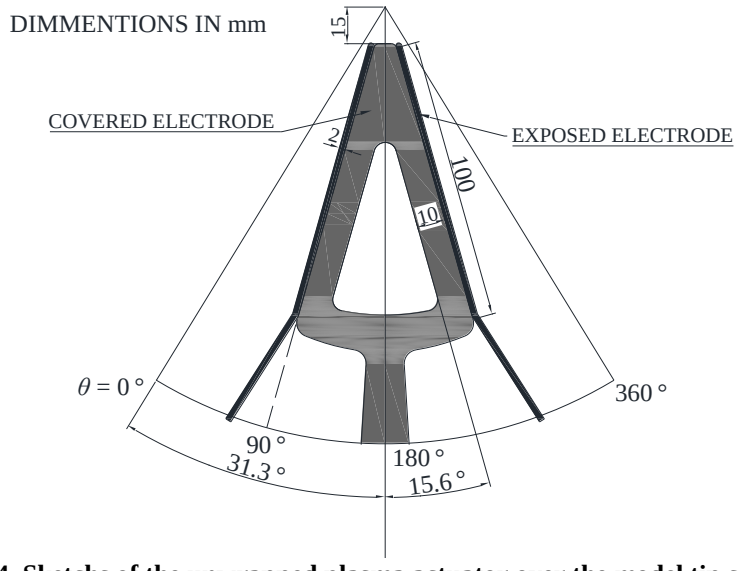

Figure 4. Sketchs of the unwrapped plasma actuator over the model tip surface.

The joint of the exposed electrode and covered electrode is just at the line of the azimuth angle $\theta = \pm 90^{\circ}$. So the affect area of the plasma actuator is just near the flow separation place, a small perturbation can contributes much to the flow field. The design idea for the position and the induced flow direction is intended to affect the boundary-layer separation positions via a plasma-induced Coanda effect. The actuator's leading edge is 15 mm to the apex of the cone. The actuator is hand-made and attached directly to the surface of the cone with no allowance. Fig. 4 shows

the sketch of the unwrapped plasma actuators before glued around the model tip surface.

D. Repetitive Nanosecond pulses Generator and Actuator Characterization

The Nanosecond generator is a high voltage power supplies and is designed to produce voltage pulses with maximum amplitude of up to 20 kV if the load is about 200-500 Ohm. The maximum of the frequency is 20 kHz. In theory, the time to reach the maximum is about 2 - 3 ns and the pulse duration at 50% is about 8 - 10 ns. The energy in each pulse is 15 mJ. Repetitive Nanosecond generator is connected to the actuator which is on the surface of the cone directly by a power line up to about 2 m. The input voltage and frequency can be controlled respectively by the knob on the generator.

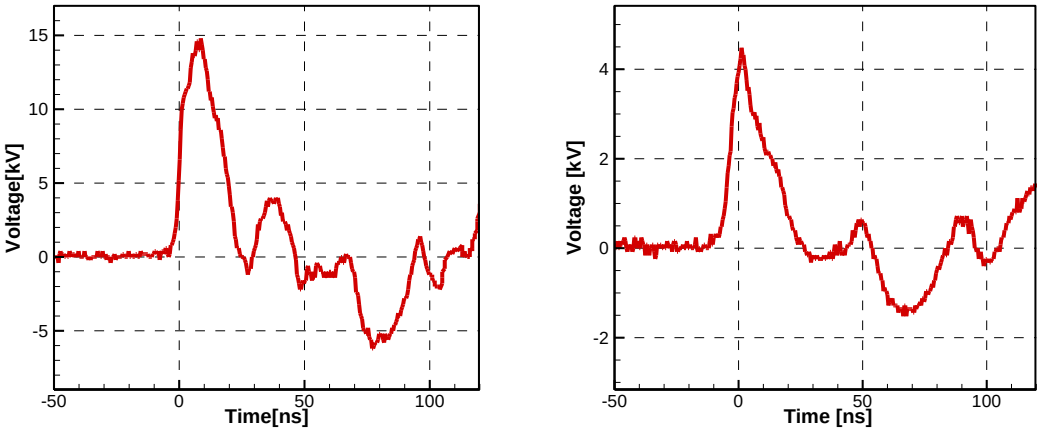

a) The maximum voltage **b) The minimum voltage**

Figure 5. Actuator voltage waveform

Figure 5 shows the voltage waveform of the NS-DBD pulse in the test. The voltage is measured by a Tektronix P6015A high voltage probe and a Tektronix DPO3054 oscilloscope. The probe is directly putted on the exposed electrode during the test. The maximum voltage of the discharge in the test is about 14.8 kV (Fig. 5a)) and the minimum output voltage of the generator is 4.48 kV (Fig. 5b)). The difference is existed between the theoretical and actual maximum voltage for the reason that the voltage is related to the load and the load of actuator in the test is not 200-500 Ohm.

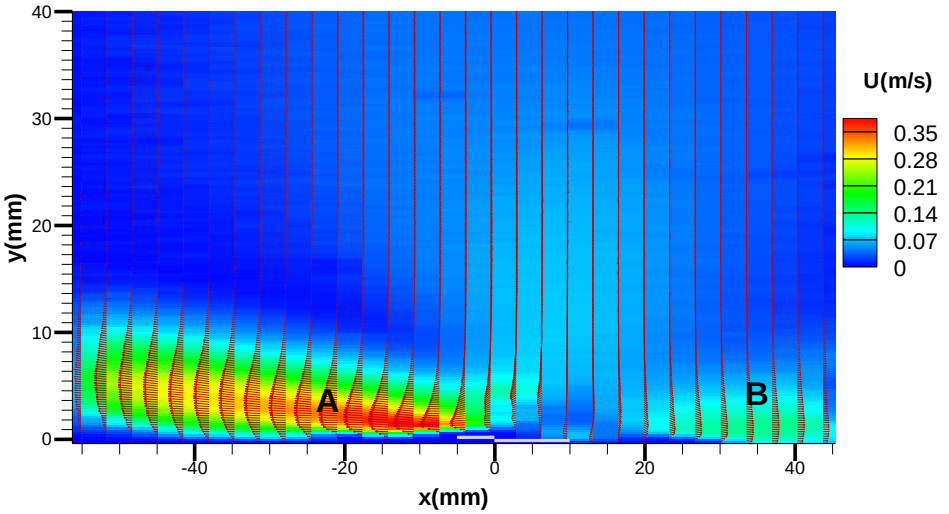

Figure 6. Time-averaged velocity vectors and contours produced by actuator over a platform. V_{max} = 9.8 kV

Fig. 6 shows the PIV study of NS-DBD on the platform and it presents that the NS-DBD effects flow field around the plasma actuator. The highest speed of the induced flow field is about 0.3883 m/s and it is much smaller than the velocity of the flow induced by the AC-DBD which reaches about 3 – 4 m/s. We define that the direction from exposed electrode to covered electrode is the potential direction and the opposite direction is the inverse

potential direction. The speed of the induced area in inverse potential direction (A) is higher than the inverse potential direction (B). After comparing with the AC-DBD, the result indicates that the NS-DBD cannot affects the flow field just by inject the velocity vector.

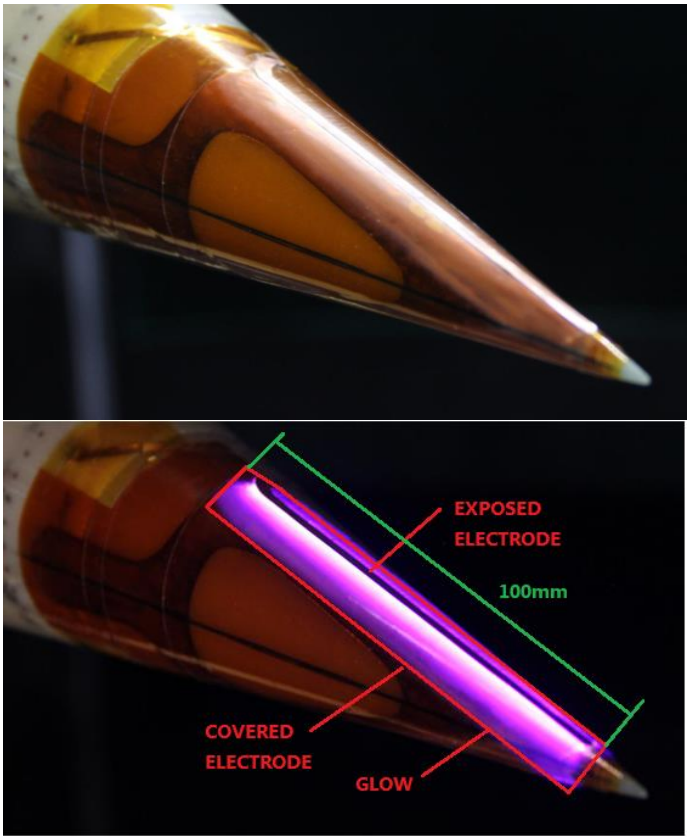

Figure 7. Images of the glow of NS-DBD on the surface of cone apex at V_{max} = 14.6 kV

Fig. 7 presents the glow of NS-DBD with a high voltage 14.6 kV on the apex, the glow is from exposed electrode to the covered electrode and has a transition from bright to normal purple. The glow which is just on the joint of the two electrodes is the brightest. The discharge glow lay over the covered electrode. The brighter and larger the glow area is, the more energy the discharge produced. The photo is taken by digital camera and the exposure time is 0.6 s and the aperture is 5.

E. Time-Averaged Pressure Measurements

The model of pressure taps is 9816 by the PSI Company with an accuracy of up to ± 0.05% FS, which are read at frequency of 50 Hz. The test time is 10 s, so we totally get 500 groups of data. The final pressure is the average of 500 times. The local side forces are calculated from the measured pressures. The sectional side-force coefficient C_{Yd} is normalized with the local diameter d and is positive when pointing to the starboard side of the cone.

The measured value is ensemble-time-average. They are measured at one section which is 331.3 mm to the tip of the model, since the pressure distribution over the forebody at angle of attack of 45° is approximately conical except in the immediate neighborhood of the body apex[15]. In Tang's paper[15], at α = 35°- 45°the pressure is approximately a constant at a given meridian angle and, thus, the pressure distribution over the cone surface is essentially conical (Fig. 8). So we can obtain the lateral force over a forebody of the cone through only on section at experiment angle of attack α = 45°.

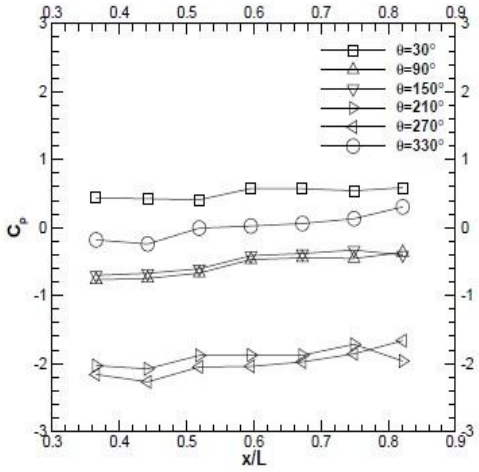

Figure 8. Pressure distributions along cone axis under port-side plasma actuation at α = 45°

F. Test Conditions

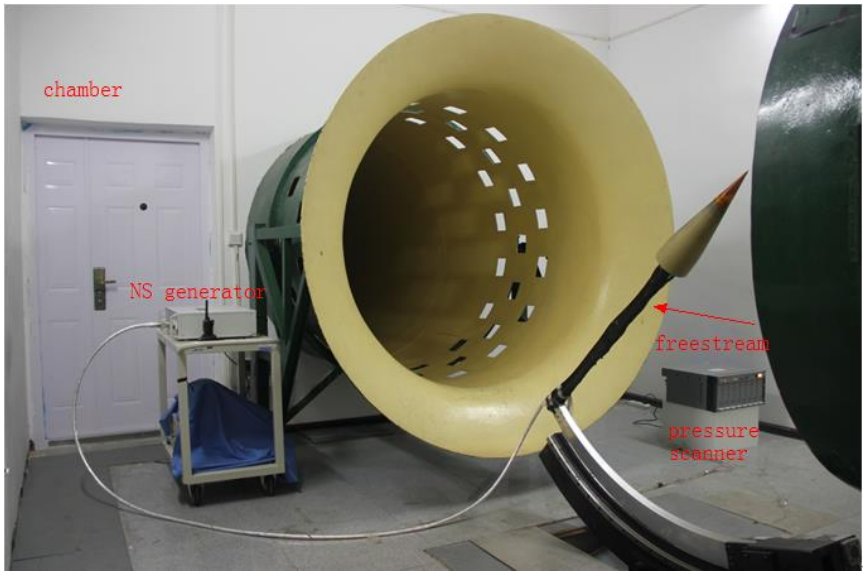

Figure 9. Model in low acoustic wind tunnel test-section photo

The experiments are performed in low acoustic wind tunnel. We choose the wind speed 22 m/s and 42 m/s. During wind tunnel test, in order to reduce the losses of power on line which is connects the actuator and generator, a tester is responsible for operating the NS generator in the chamber (Fig. 9) far away from the flow field and test section. The pressure scanner is set on the other side and connected with the outside operate computer by a cable. The pressure scanner is set far away from the NS generator and actuator in case of being inference by electromagnetic.

III. Experimental Results

A. Baseline Verification

In order to insure the setup of the model is accurate and the man-made actuator is up to standard, we do some tests at small angles of attack. The test angle of attack is α = 0°, 5°, 10°, 15° and 20°, the test wind speed is 42 m/s. The calculation results are shown in Fig. 11. For 5 degrees, the pressure distribution on port and starboard side is approximately symmetrical and the suction peak on both sides is nearly the same. However, the pressure distribution of 5° is not completely symmetrical. The reason is concluded to the problem of manual actuator, and we boil it down to the reasonable error.

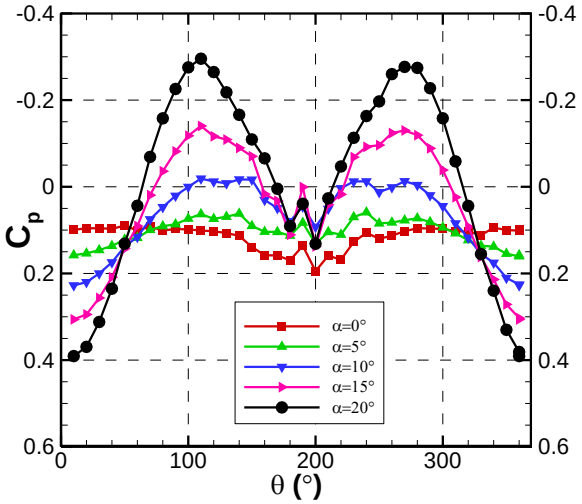

Figure 10. Model symmetry test at 42 m/s, *Re* = 3.09 × 10^5.

B. Comparison of Plasma-Off and Plasma-On results at 22 m/s (*Re* = 1.64 × 10^5)

The pressure distributions are presented in Fig. 11 for plasma off, plasma port-on and plasma starboard-on, respectively. Based on Fig. 11, pressure distributions of plasma off are apparently asymmetric and the suction peak of the starboard side is higher than the port side. When starboard actuator working, it weakly increase the port side pressure and decrease the other side, shown in Fig. 11 b). When port actuator working, it increase the starboard side pressure. Even though the value of the lateral side force C_{Yd} is different, the sign of the C_{Yd} of port and starboard on is not opposite. The lateral force and separation position θ_p and θ_s is listed in Table 1.

Fig. 11 also gives us some information about the station of the two asymmetric vortices. No matter plasma on or off, the starboard side vortices is closer to the model surface and the port side one is far away from the model surface. When port on, it pulls the port vortex closer and pushes the starboard vortex away, but the starboard vortex is still closer to the surface than port side one. So the control of the plasma at 22 m/s is limited.

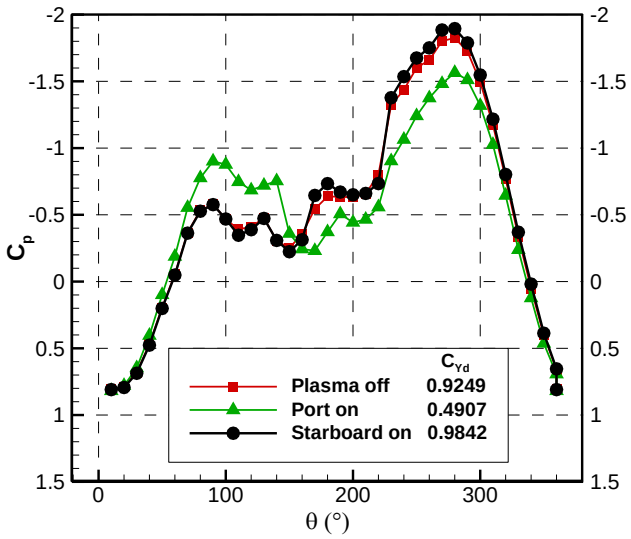

a) Azimuth angle 0° - 360°

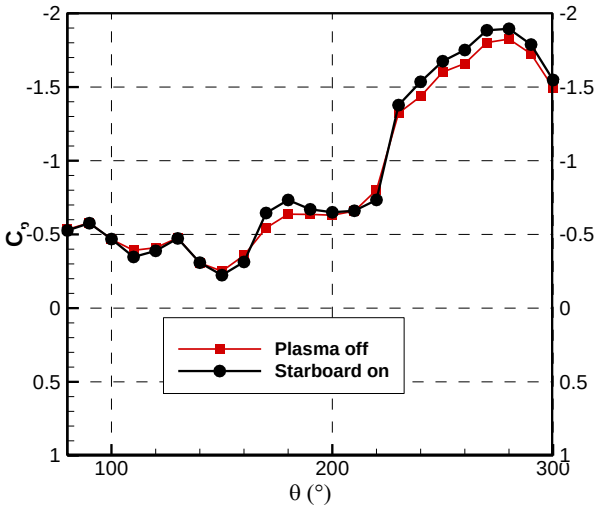

b) Azimuth angle 80° - 300°

Figure 11. Pressure distributions under steady actuation, V_{max} = 15.6 kV, F = 2.8 kHz, α =45°

Table 1. Separation position θ_p and θ_s of the measure station, U_∞ = 22 m/s.

Mode	θ_p	θ_s	C_{Yd}
Plasma Off	110°	-150°	0.9249
Port-on	120°	-150°	0.4907
Starboard-on	110°	-150°	0.9842

C. Convergence of Time-Average Pressures at 22 m/s (Re = 1.64 × 10^5)

During the experiment, a tester is responsible for manipulating the acquisition system. A proper time delay is needed before the acquisition, the flow field should be steady before starting gathering the data. In order to show that the results presented above are convergent and believable, a time-average pressure calculation test is performed. The test choose 6 points every 60° of the total 36 pressure-tappings around the test section (0°, 60°, 120°, 180°, 240°, 300°). At every angle picked before, the test time is divided on average, 1s for each. The calculation result is shown in Fig.13 for plasma off, plasma port-on and plasma starboard on. The C_p curve is approximately parallel to the x axis as the time goes on. So, it indicates that the flow field is steady, acquisition is correct the data is believable.

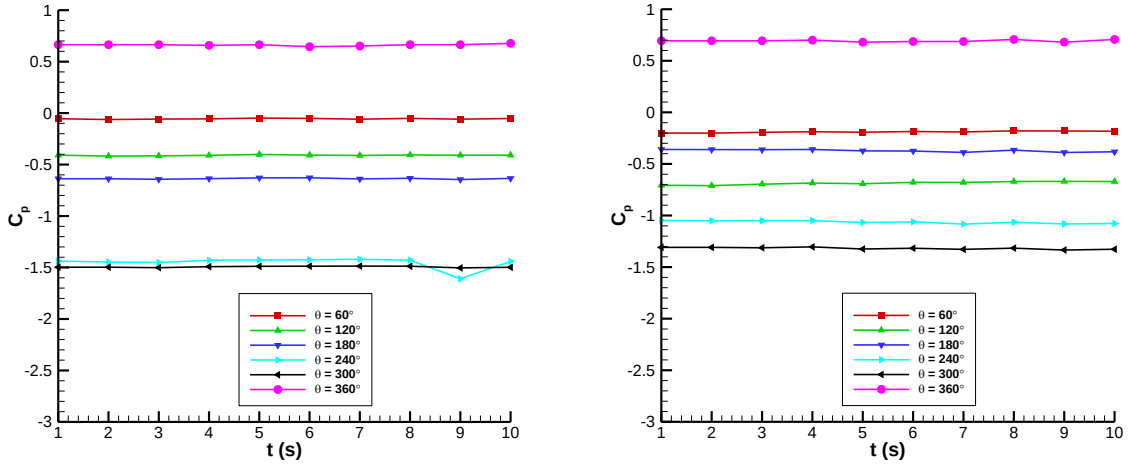

a) Plasma off b) Port on

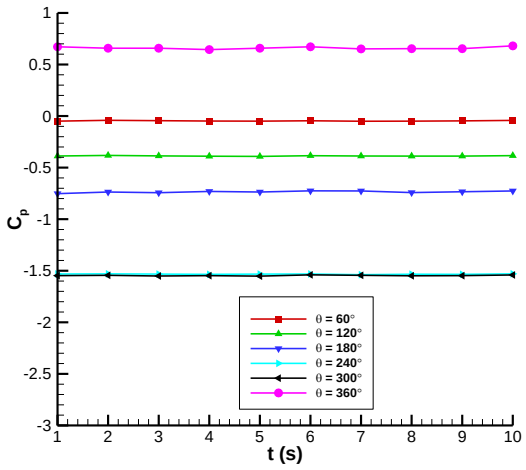

c) Starboard on

Figure 12. Convergence of Time-Average Pressure, V_{max}=15.6 kV, F=2.8 kHz, α =45°.

D. Comparison of Plasma-Off and Plasma-On results at 42 m/s (Re = 3.09 × 10^5)

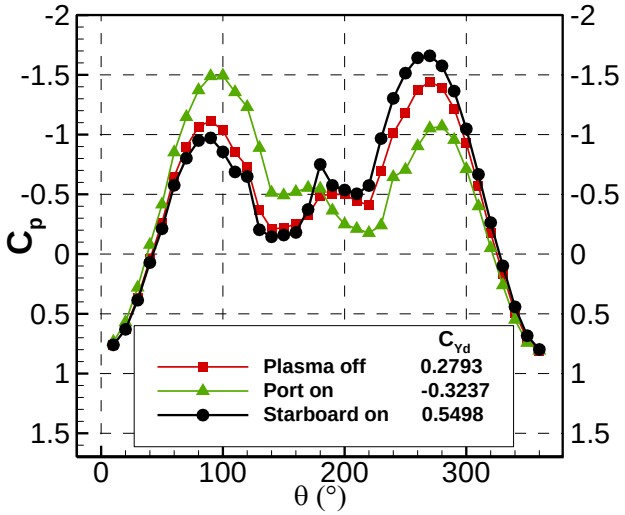

Figure 13. Pressure distributions under steady actuation, V_{max}=14.6 kV, F=3.8 kHz, α =45°

Table 2. Separation position θ_p and θ_s of the measure station, U_∞ = 42 m/s.

Mode	θ_p	θ_s	C_{Yd}
Plasma Off	140°	-140°	0.2793
Port-on	150°	-130°	-0.3237
Starboard-on	140°	-140°	0.5498

The pressure distributions of 42 m/s wind speed are presented in Fig. 13 for plasma off, plasma port-on and plasma starboard-on, respectively. The flow which is induced by the port on actuation and starboard on actuation are both decrease the pressure on actuating side and increase the pressure on the other side. During plasma off and starboard on, the suction peak of the starboard side is higher than which on the port side. The position of the suction peak also predicts the position of the asymmetry vortex. At 42 m/s, the port on actuation pull the port side vortex to the model surface and push the starboard side vortex which is original closer to the surface far away. The location relative to the model of the port and starboard side is reversed.

The separation position θ_p and θ_s are shown in Table 2. The port on actuation delay the separation on port side and the starboard on actuation delay the separation on starboard side. The angle of delay is about 10° .

E. Convergence of Time-Average Pressures

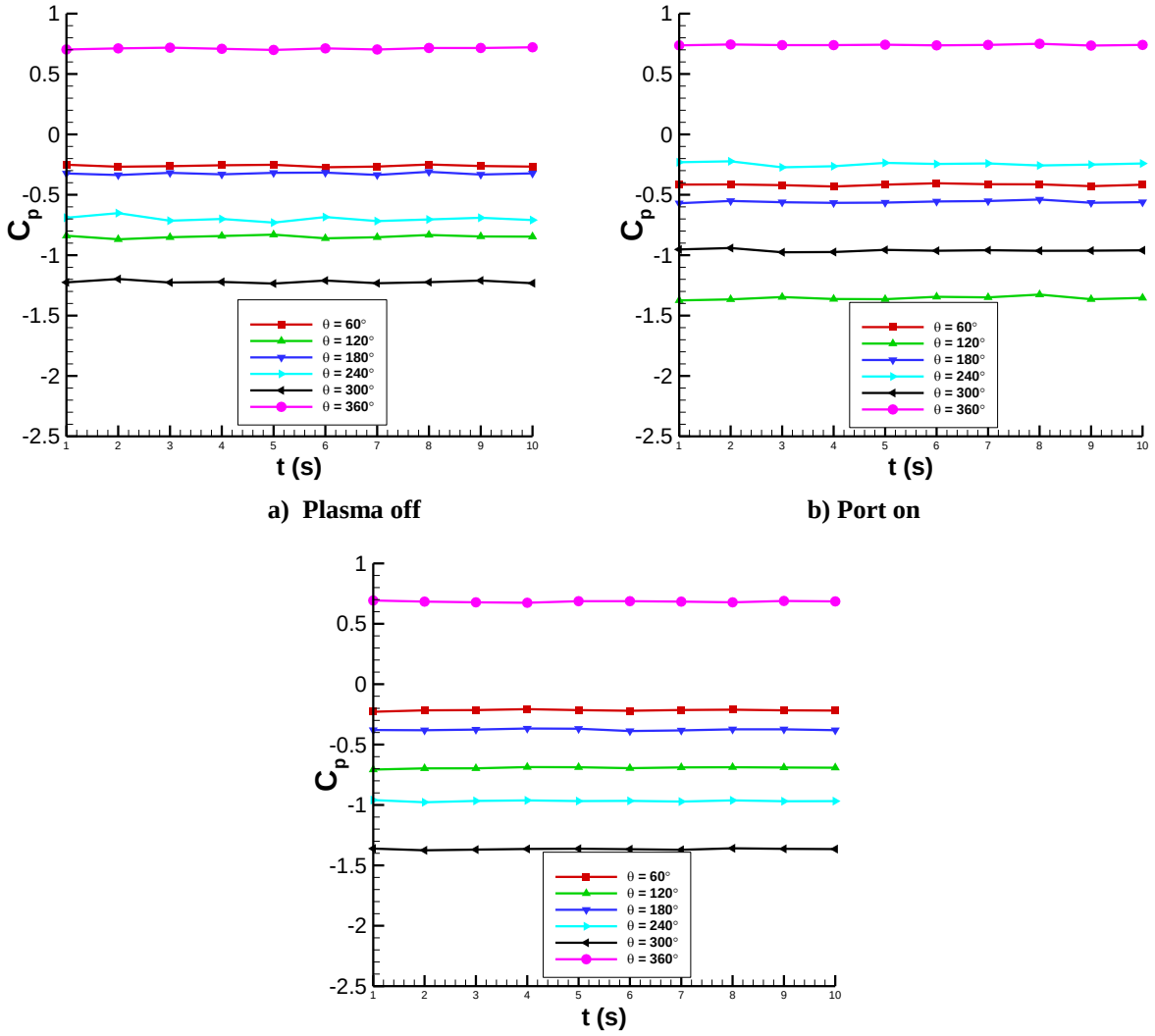

a) Plasma off **b) Port on**

c) Starboard on

Figure 14. Convergence of Time-Average Pressure, V_{max} = 14.6 kV, F = 3.8 kHz, α = 45°.

IV. Conclusion

An actuator power by a new kind of repetitive nanosecond pulses generator is been used in the study of the control of lateral force and asymmetric vortex over a slender circular conical forebody at high angle of attack and higher wind speed. A pair of plasma actuators is placed along the two opposite side rays of the conical forebody near its apex at an angle of attack of 45° with arrangement used in this paper, freestream velocity is 22 m/s and 42 m/s with the Reynolds number 1.64×10^5 and 3.09×10^5 based on the cone base diameter. The pressure distribution of plasma off, port-on and starboard-on at test section of the forebody is obtained, and the lateral force of the cone is calculated from the pressure distribution by integration. The pressure distributions are measured by the time-averaged pressure scanner whose sample rate is 50 Hz.

The final result of the flow control test suggest that the port on and starboard on actuation both decrease the pressure of the actuating side and increase the pressure of the other side. At 22 m/s, the test voltage and frequency is 15.6 kV and 2.8 kHz. The port on actuation only pull the port vortex a limited distance to the model surface, which is far from enough to reverse asymmetric vortices. The energy that port actuation inject into the boundary layer is not enough, so it cannot control the asymmetric vortices. At 42 m/s, the test voltage and frequency is 14.6 kV and 3.8 kHz. Plasma actuating makes the same side suction peak higher than the other side. Although the pressure distribution of actuation discharge is not mirror reversed, the final lateral force of the port on and starboard on is

opposite in sign and the absolute value is close. So we concluded that the NS-DBD actuating has the ability to control the asymmetric vortex over a cone forebody at high wind speed 42 m/s.

V. Future work

There will be more study on the characteristic and mechanism of the NS-DBD and also an optimized arrangement of the actuator are needed. There are some advanced technologies which can be adopted in the study of NS-DBD, like Schlieren technology. The compression wave of NS-DBD is the key point for explaining the mechanism of the NS-DBD.

Why the NS-DBD can only works at a higher wind speed is an important problem. More detail work is needed for further study to detect and analyze flow field over the cone through PIV technology. By PIV technology, a clear and accurate flow filed will be displayed and then combined with the pressure distribution, the flow field and the effect of NS-DBD actuator can be studied across the board. We can also do some research on analysis of the separation point of the vortex.

Acknowledgments

The present work is supported by *National Natural Science Foundation of China* (11172243, 51107101), *the Foundation for Fundamental Research of the Northwestern Polytechnical University* (JC201218). The authors would like to express their gratitude to Professor Huaxing Li and Xuanshi Meng in NPU for their valuable contribution and acknowledge Haiyang Hu and Xuzhao Han of Northwestern Polytechnical University for their technical support in the wind-tunnel tests.

References

[1]Ericsson L., "Sources of high alpha vortex asymmetry at zero sideslip," *Journal of Aircraft*, Vol. 29, No. 6, 1992, pp. 1086-1090.

[2]Zilliac G. G., Degani D. and Tobak M., "Asymmetric vortices on a slender body of revolution," *AIAA J.*, Vol. 29, No. 5, 1991, pp. 667-675.

[3]Levy Y., Hesselink L. and Degani D., "Systematic Study of the Correlation Between Geometrical Disturbances and Flow Asymmetries," *AIAA J.*, Vol. 34, No. 4, 1996, pp. 772–777.

[4]Cai J, Tsai H, Luo S and Liu F. "Stability of Vortex Pairs over Slender Conical Bodies: Analysis and Numerical Computation," *AIAA J.*, Vol. 46, No. 3, 2008, pp: 712–722.

[5]Malcolm, G., "Forebody Vortex Control: A Progress Review," *AIAA Paper* 93-3540, Aug. 1993.

[6]Williams D., "A Review of Forebody Vortex Control Scenarios," *AIAA Paper* 97-1967, June 1997.

[7]Post, M., and Corke, T. C., "Separation Control on High Angle of Attack Airfoil Using Plasma Actuators," *AIAA J.*, Vol. 42, No. 11, Nov. 2004, pp. 2177–2184.

[8]Post, M., and Corke, T. C., "Separation Control Using Plasma Actuators: Dynamic Stall Vortex Control on Oscillating Airfoil," *AIAA J.*, Vol. 44, No. 12, Dec. 2006, pp. 3125–3135.

[9]Huang, J., Corke, T. C., and Thomas, F. O., "Plasma Actuators for Separation Control of Low-Pressure Turbine Blades," *AIAA J.*, Vol. 44, No. 1, Jan. 2006, pp. 51–57.

[10]Corke, T. C., and Post, M., "Overview of Plasma Flow Control: Concepts, Optimization, and Applications," *AIAA Paper* 2005-563, Jan. 2005.

[11]Takashi Matsuno, Hiromitsu Kawazoe and Robert C. Nelson. "Aerodynamic Control of High Performance Aircraft Using Pulsed Plasma Actuators," *AIAA Paper* 2009-697, Jan. 2009.

[12]Meng X, Wang J, Cai J, Luo S and Liu F. "Optimal DBD Duty-Cycle for Conical Forebody Side-Force Proportional Control." *AIAA Paper*2013-0347, Jan. 2013.

[13]Jesse Little, Keisuke Takashima and Munetake Nishihara. "Separation Control with Nanosecond-Pulse-Driven Dielectric Barrier Discharge Plasma Actuators," *AIAA J.*, Vol. 50, No. 2, Feb. 2012, pp. 350–365.

[14]Keisuke Takashima, Yvette Zuzeek and Walter R. Lempert. "Characterization of Surface Dielectric Barrier Discharge Plasma Sustained by Repetitive Nanosecond Pulses," *AIAA Plasmadynamics and Laser Conference* 28 June-1 July 2010/Chicago, IL.

[15]Huarui Tang, Zijie Zhao, Huaxing Li, Feng Liu and Shijun Luo, "Flow Asymmetry over a Conical Forebody under Plasma Actuation," *AIAA Paper* 2010-4838, Jun., 2010.